AMERICAN SOCIETY FOR MICROBIOLOGY | mSphere®

RESEARCH ARTICLE

A Conserved Machinery Underlies the Synthesis of a Chitosan Layer in the *Candida* Chlamydospore Cell Wall

Leo D. Bemena,[a] Kyunghun Min,[b] James B. Konopka,[b] Aaron M. Neiman[a]

[a]Department of Biochemistry and Cell Biology, Stony Brook University, Stony Brook, New York, USA
[b]Department of Microbiology and Immunology, Stony Brook University, Stony Brook, New York, USA

ABSTRACT The polysaccharide chitosan is found in the cell wall of specific cell types in a variety of fungal species where it contributes to stress resistance, or in pathogenic fungi, virulence. Under certain growth conditions, the pathogenic yeast *Candida dubliniensis* forms a cell type termed a chlamydospore, which has an additional internal layer in its cell wall compared to hyphal or yeast cell types. We report that this internal layer of the chlamydospore wall is rich in chitosan. The ascospore wall of *Saccharomyces cerevisiae* also has a distinct chitosan layer. As in *S. cerevisiae*, formation of the chitosan layer in the *C. dubliniensis* wall requires the chitin synthase *CHS3* and the chitin deacetylase *CDA2*. In addition, three lipid droplet-localized proteins—Rrt8, Srt1, and Mum3—identified in *S. cerevisiae* as important for chitosan layer assembly in the ascospore wall are required for the formation of the chitosan layer of the chlamydospore wall in *C. dubliniensis*. These results reveal that a conserved machinery is required for the synthesis of a distinct chitosan layer in the walls of these two yeasts and may be generally important for incorporation of chitosan into fungal walls.

IMPORTANCE The cell wall is the interface between the fungal cell and its environment and disruption of cell wall assembly is an effective strategy for antifungal therapies. Therefore, a detailed understanding of how cell walls form is critical to identify potential drug targets and develop therapeutic strategies. This study shows that a set of genes required for the assembly of a chitosan layer in the cell wall of *S. cerevisiae* is also necessary for chitosan formation in a different cell type in a different yeast, *C. dubliniensis*. Because chitosan incorporation into the cell wall can be important for virulence, the conservation of this pathway suggests possible new targets for antifungals aimed at disrupting cell wall function.

KEYWORDS cell wall, chitin synthase, chitin deacetylase, lipid droplet, chlamydospore

The cell wall is the interface between the fungal cell and the environment (1). In pathogenic fungi, the cell wall is critical for virulence as it mediates interactions with, and evasion of, the host immune system (2). Fungal cell walls are essential for viability and are a common target of antifungal drugs (3–6). Therefore, understanding the structure and assembly of the fungal wall is important for the development of antifungal therapies.

Fungal cell walls are composed primarily of heavily mannosylated proteins (referred to as mannan) and polysaccharides (1). In particular β-1,3 glucans and chitin, a β-1,4-*N*-acetylglucosamine polymer, are common structural components of fungal cell walls (1, 7, 8). Chitosan, a β-1,4-glucosamine polymer created by deacetylation of chitin, is also found in fungal cell walls but is often limited to specific cell types or developmental stages (9–12). The presence of chitosan in cell walls can be critical for the organism. For example, in the pathogen *Cryptococcus neoformans* chitosan in the wall dampens the host inflammatory response, and *Cryptococcus* strains unable to synthesize

Citation Bemena LD, Min K, Konopka JB, Neiman AM. 2021. A conserved machinery underlies the synthesis of a chitosan layer in the *Candida* chlamydospore cell wall. mSphere 6:e00080-21. https://doi.org/10.1128/mSphere.00080-21.

Editor Aaron P. Mitchell, University of Georgia

Address correspondence to Aaron M. Neiman, aaron.neiman@stonybrook.edu.

Received 25 January 2021
Accepted 2 April 2021
Published 28 April 2021

chitosan are avirulent (13–15). Chitosan is often found in conjunction with polyphenolic compounds, which has led to the proposal that chitosan-polyphenol complexes are a conserved architectural motif in fungal walls (16).

How chitosan is incorporated into the cell wall is not yet well understood. This process has been best studied in the budding yeast, *Saccharomyces cerevisiae*, where chitosan is found uniquely in the walls of ascospores, a dormant cell type produced after meiosis by a process termed sporulation (17, 18). The ascospore wall consists of four distinct layers, named for their primary constituents, which are deposited in a sequential manner: mannan, glucan, chitosan, and dityrosine (10, 19–22). The mannan and glucan layers form the inner layers of the ascospore wall and are similar in composition to layers in the vegetative cell wall (21). The outer ascospore wall, containing a layer of chitosan and a layer of the polyphenol dityrosine, is unique to ascospores and confers resistance against environmental insults (10, 23, 24).

The chitin in the vegetative cell wall of *S. cerevisiae* is produced by three different chitin synthases, Chs1, -2, and -3 (25–27). However, during sporulation chitin is produced exclusively by Chs3 (28). Chitosan is generated when acetyl groups on chitin are removed by the sporulation-specific deacetylases, Cda1 and Cda2 (11, 29). Deletion of both *CDA1* and *CDA2* results in spore walls that contain chitin but lack the chitosan layer. In addition, while the mannan and beta-glucan layers are present, the dityrosine layer is missing. Chitosan is therefore necessary for the formation of both layers of the outer cell wall (29). In contrast, formation of the chitosan layer is independent of the formation of dityrosine. Dityrosine is synthesized from L-tyrosine in the spore cytosol by the sequential action of the Dit1 and Dit2 enzymes (30), and mutants in either *DIT1* or *DIT2* result in loss of the dityrosine without any obvious effect on the chitosan layer (23).

In addition to the genes directly involved in chitosan or dityrosine synthesis, several other genes are required for the formation of one or more layers of the outer spore wall (31–35). Genes of unknown function such as *MUM3* and *OSW1*, as well as the *cis*-prenyltransferase encoded by *SRT1*, lack both the chitosan and dityrosine layers (34). In an *srt1*Δ mutant, Chs3 activity is reduced, suggesting that Srt1 contributes to spore wall formation through regulation of Chs3 (34). Srt1 is localized to a class of lipid droplets that is physically associated with the developing spore wall (34, 36). Mutants in the paralogous genes *LDS1*, *LDS2*, and *RRT8*, which encode lipid droplet-localized proteins, are specifically defective in the dityrosine layer (35). Whether the genes required for chitosan layer formation in *S. cerevisiae* are functionally conserved in other fungi has not been reported.

The human fungal pathogen *Candida albicans* and its close relative, *Candida dubliniensis*, exhibit cell types with various morphologies (37, 38). Although these *Candida* species are not known to produce ascospores, under certain conditions they produce a distinct, thick-walled cell type at hyphal tips termed a chlamydospore (37, 39). Chlamydospores are large round cells that are the result of mitotic divisions, unlike ascospores, which package the haploid products of meiosis. The function of chlamydospores in the *Candida* life cycle is unknown. Nutrient limitation or low-oxygen conditions are often required to induce the appearance of chlamydospores, and *C. dubliniensis* appears to undergo chlamydosporulation more readily than *C. albicans* (40, 41).

Ultrastructural studies revealed that the chlamydospore wall is more extensive than the wall of budding or hyphal *C. dubliniensis* cells with an internal layer not found in those cell types (42). The structure and composition of this layer has not been well characterized. In the present study, we investigated the organization of the chlamydospore wall in *C. dubliniensis*. This study demonstrated that the unique internal layer of the chlamydospore wall is composed of chitosan. Moreover, genes encoding orthologs of *S. cerevisiae* proteins necessary for chitosan layer synthesis in ascospores are also required chlamydospore wall assembly. These results reveal that a conserved pathway underlies chitosan synthesis and incorporation in these two yeasts.

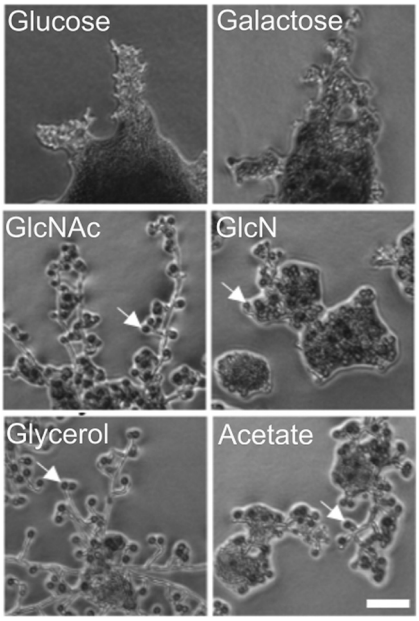

FIG 1 Effect of different carbon sources on the chlamydospore formation. A wild-type *C. dubliniensis* strain (Cd1465) was spotted on synthetic agar medium containing the indicated carbon sources and photographed on agar after 24 h of growth. Gal, galactose; GlcNAc, *N*-acetylglucosamine; GlcN, glucosamine. White arrows highlight examples of chlamydospores. Scale bar, 50 nm.

RESULTS

***C. dubliniensis* forms chlamydospores on solid medium containing nonfermentable carbon sources.** In examining the growth of clinical isolates of *C. dubliniensis*, we discovered that growth on certain carbon sources induced chlamydospore formation. While chlamydospores were not observed in cultures grown on synthetic medium containing glucose or galactose, growth on *N*-acetylglucosamine, glucosamine, glycerol, or acetate all led to hyphal growth and the appearance of chlamydospores (Fig. 1). Three different clinical isolates of *C. dubliniensis* as well as the established *C. dubliniensis* strain SN90 (43) displayed this behavior, whereas *C. albicans* did not form chlamydospores on any of these media (K. Min, unpublished data). Solid glycerol medium was particularly efficient at inducing chlamydospores (no chlamydospores were seen in liquid medium with any carbon source) (Fig. 1). We took advantage of these induction conditions to examine the properties of the chlamydospore wall in *C. dubliniensis*, using the clinical isolate that showed the most robust chlamydospore formation.

The chlamydospore wall of *C. dubliniensis* contains chitosan but not dityrosine. In the *S. cerevisiae* ascospore wall, a layer of chitosan underlies the dityrosine layer and chitosan is found in association with polyphenol components in other fungal cell walls (9). The observation that chlamydospore walls of *C. albicans* contain dityrosine suggested that chlamydospore walls might contain chitosan as well (44). Chitosan can be specifically visualized using the stain Eosin Y, which has affinity for chitosan but not chitin (9, 35). When *C. dubliniensis* chlamydospores were stained with Eosin Y and examined by fluorescence microscopy, bright Eosin Y-dependent fluorescence was visible at the periphery of the chlamydospore (Fig. 2). The fluorescent signal was not observed on hyphal cells, consistent with the presence of chitosan specifically in the chlamydospore wall. Similar staining of *C. albicans* chlamydospores with Eosin Y has recently been reported (45).

To prove whether Eosin Y staining was specifically detecting chitosan, a genetic approach was used. The *C. dubliniensis* genome encodes one member of the chitin deacetylase enzyme family, Cda2 (Cd36_25340), required to convert chitin to chitosan. If Eosin Y staining is due to the presence of chitosan in the chlamydospore wall, then this staining should be reduced or absent in a *cda2* deletion that lacks chitin deacetylase activity (9, 35).

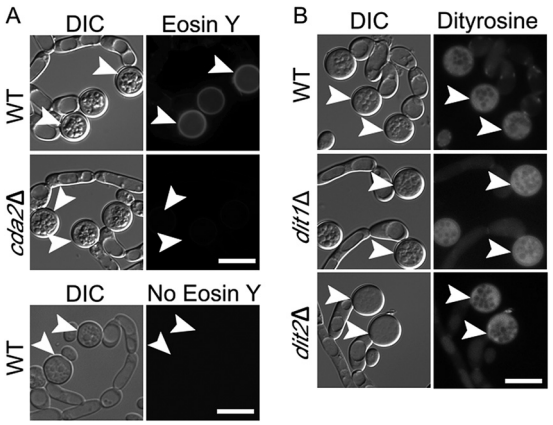

FIG 2 Fluorescence analysis of the chlamydospore wall of *C. dubliniensis*. (A) Chlamydospores of WT (Cd1465) and *cda2*Δ (BEM7) strains were stained with Eosin Y to visualize the chitosan layer and imaged using a GFP filter set. Wild-type (WT) chlamydospores with no Eosin Y staining are shown as control. (B) WT (Cd1465), *dit1*Δ (BEM9), or *dit2*Δ (BEM10) strains were grown on SG medium to induce chlamydospores and then visualized by differential interference contrast (DIC) or fluorescence microscopy using a dityrosine filter set (excitation [Ex.], 320 nm; emission [Em.], 410 nm). Arrowheads indicate examples of chlamydospores visible in the images. Scale bar, 10 μm.

C. dubliniensis is a diploid organism. To generate a *cda2*Δ/*cda2*Δ deletion strain in *C. dubliniensis*, we utilized a transient CRISPR-Cas9 system originally developed for *C. albicans* (46). Double-strand breaks in the two *CDA2* alleles were generated by CRISPR-Cas9 and used to target integration of a SAT1 cassette (47), which confers resistance to the drug nourseothricin (NAT), into the *CDA2* locus. By selecting for NAT-resistant transformants, diploids homozygous for *cda2*Δ were obtained. Chlamydospore formation was induced in the *cda2*Δ/*cda2*Δ diploid on glycerol medium and examined by Eosin Y staining. No Eosin Y staining was observed, confirming the presence of chitosan in the wild-type chlamydospore wall (Fig. 2A).

To test whether the chlamydospore wall of *C. dubliniensis* also contains dityrosine, chlamydospores were analyzed by fluorescence microscopy using a filter cube optimized for dityrosine (48). Unlike earlier reports in *C. albicans*, no fluorescence was seen specifically in the cell wall, though fluorescence was visible throughout the cytoplasm that was brighter than background fluorescence in the hyphal cells (Fig. 2B). This fluorescence is not due to dityrosine, however, since deletion of the *C. dubliniensis DIT1* or *DIT2* genes (which are required for making dityrosine in budding yeast) also exhibited the cytoplasmic fluorescence (Fig. 2B). Therefore, a common feature in chlamydospores from *C. dubliniensis* and *C. albicans* and the ascospores from budding yeast is the presence of a chitosan layer in the cell wall.

The chlamydospore wall of *C. albicans* also lacks dityrosine fluorescence. The lack of dityrosine fluorescence in the *C. dubliniensis* chlamydospore wall led us to examine *C. albicans* chlamydospores under our microscopy conditions. Cells were spread on a corn meal agar plate and a glass cover slip placed on top of the cells. Chlamydospores were examined after 5 days incubation as described previously (44). Using a filter set similar to what was used in reference 44, we also see a distinct fluorescence signal from the chlamydospore wall (Fig. 3). However, using a filter set optimized for dityrosine excitation and emission, the *C. albicans* chlamydospores display a diffuse fluorescence throughout the cytoplasm, as in *C. dubliniensis*. Also similar to *C. dubliniensis*, the *C. albicans* chlamydospores stain brightly with Eosin Y. Thus, the *C. albicans* chlamydospore wall appears identical to *C dubliniensis*, suggesting that the wall fluorescence seen under UV illumination is not due to dityrosine.

A chitosan synthesis pathway is conserved in *C. dubliniensis*. *S. cerevisiae* encodes three different chitin synthases, but chitin synthase 3 (*CHS3*) is specifically used in the synthesis of the chitosan layer of the spore wall (28). *C. dubliniensis* encodes four different predicted chitin synthases, and the ORF Cd36_12160 encodes the ortholog of

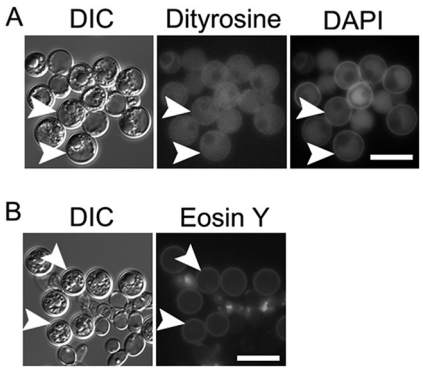

FIG 3 Fluorescence analysis of the *C. albicans* chlamydospore wall. (A) Unstained chlamydospores of *C. albicans* strain NLC1 were imaged using either a dityrosine filter set (Ex., 320 nm; Em., 410 nm) or a DAPI filter set (Ex., 375 nm; Em., 475 nm). (B) Chlamydospores of NLC1 stained with Eosin Y and imaged using a GFP filter set. Arrowheads indicate examples of chlamydospores visible in the images. Scale bar, 10 μm.

S. cerevisiae CHS3 (49, 50). To examine whether the use of the Chs3 ortholog for chitosan synthesis is conserved, a *C. dubliniensis chs3*Δ/*chs3*Δ mutant was constructed, and chlamydospores were stained with Eosin Y. Interestingly, as for the *cda2*Δ/*cda2*Δ mutant, greatly reduced fluorescence signal from the Eosin Y staining was seen in the *chs3*Δ/*chs3*Δ chlamydospore wall (Fig. 4A). In *S. cerevisiae*, the ascospore wall does not stain with the dye Calcofluor White (CFW), but deletion of *CDA1* and *CDA2* leads to the accumulation of chitin in the ascospore wall and bright CFW staining (29). In contrast, in *C. dubliniensis*, deletion of *CDA2* or *CHS3* leads to, at best, a modest increase in staining around the cell wall (Fig. 4A). In the mutant and wild-type strains, CFW predominantly stains the septa, consistent with earlier reports in *C. albicans* that chitin at the septum is deposited by chitin synthase 2 (51) (Fig. 4A). In sum, these results indicate that Chs3 and Cda2, the same enzymes that generate chitosan in ascospores, collaborate to generate chitosan in the chlamydospore wall.

C. dubliniensis encodes uncharacterized orthologs for several of genes required for making ascospore outer cell walls. If the process of chitosan assembly in the wall is conserved, then these same genes may function in chitosan deposition into the chlamydospore wall as well. In particular, we focused on the orthologs of *S. cerevisiae MUM3* (Cd36_82000), *SRT1* (Cd36_11510), and *RRT8* (Cd36_33980). Homozygous deletions for all three of the *C. dubliniensis* genes were constructed, and chlamydospores of the mutant strains were examined by Eosin Y and CFW staining. Relative to the wild type, the intensity of the Eosin Y fluorescence was reduced in all of the mutant strains, while the fluorescence from CFW staining was unaltered (Fig. 4A). These results are similar to the effects of *chs3*Δ and *cda2*Δ and suggest that these genes are important for chitosan formation in *C. dubliniensis*.

To more carefully assess the effect of the mutants, the fluorescence intensity of the Eosin Y staining of individual chlamydospores was categorized as bright, reduced, or absent and the number of chlamydospores in each category was scored for each strain (Fig. 4B). The *cda2*Δ/*cda2*Δ and *chs3*Δ/*chs3*Δ mutant strains displayed a sharp reduction in the fraction of chlamydospores with bright fluorescence intensity and a corresponding increase in chlamydospores displaying no Eosin Y fluorescence. As expected, mutation of *DIT1* had no obvious effect on Eosin Y staining. In contrast, the *mum3*Δ/*mum3*Δ, *srt1*Δ/*srt1*Δ, and *rrt8*Δ/*rrt8*Δ diploids all showed phenotypes similar to *chs3*Δ and *cda2*Δ strains with a significant, though not quite as strong, reduction in brightly staining spores and an increase in unstained spores (Fig. 4B).

To confirm that the loss of Eosin Y staining was due to the deletion alleles and not an off-target effect from CRISPR/Cas9, the ability of the wild-type gene to complement each mutant was tested. Each wild-type gene was cloned into the integrating plasmid

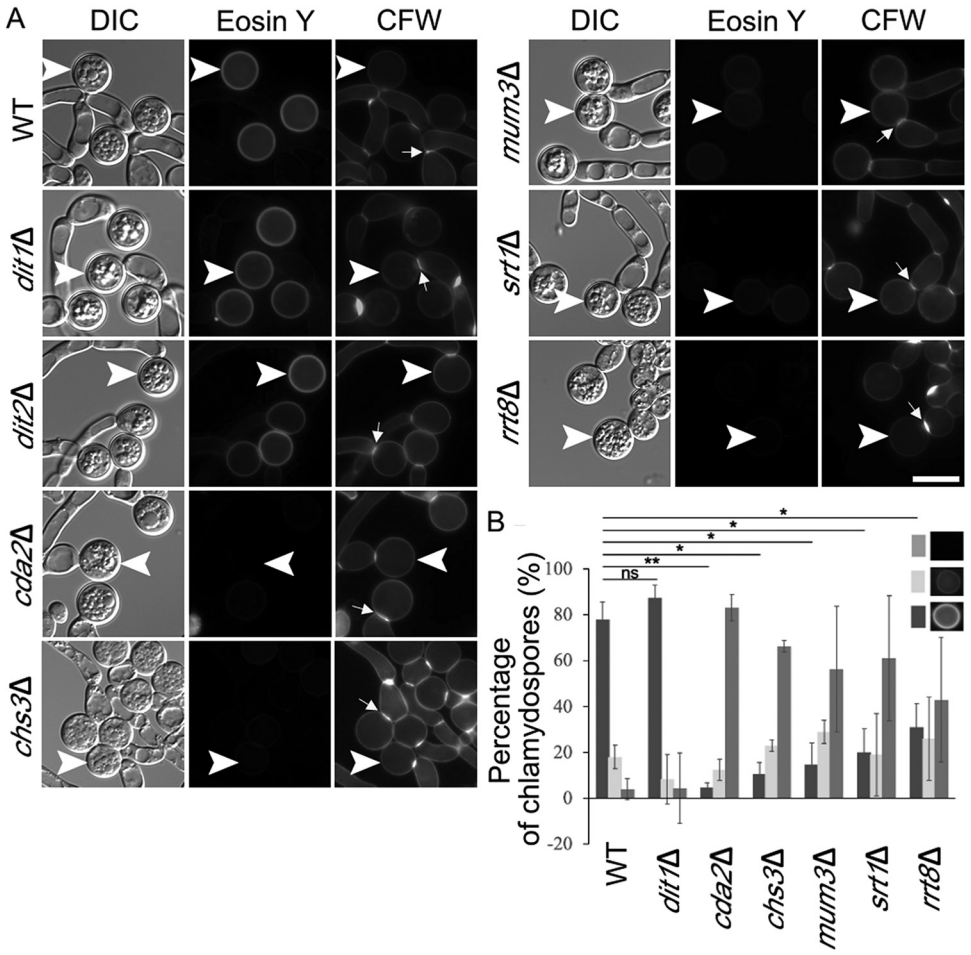

FIG 4 Effect of mutations in *C. dubliniensis* orthologs of *S. cerevisiae* spore wall genes on the chlamydospore wall. (A) Cells of strains of the indicated genotype were grown on SGlycerol medium and then stained with both Eosin Y to label chitosan and Calcofluor White (CFW) to label chitin or chitosan. Arrowheads indicate examples of chlamydospores visible in the images. Arrows indicate examples of CFW-stained septa. Scale bar, 10 μm. (B) The intensity of the Eosin Y fluorescence was categorized as bright, dim, or no fluorescence for each chlamydospore, and the number of chlamydospores in each category for each strain was quantified. For each strain, the value represents the average for 100 chlamydospores in each of three independent experiments. Error bars indicate one standard deviation. One asterisk (*) indicates significant difference at $P < 0.05$; two asterisks (**) indicates significant difference at $P < 0.0005$ (Student *t* test).

Clp10-SAT, which can be targeted to integrate into the *RPS1* locus (52). This vector uses the same *SAT1* selectable marker that was used to make the deletion alleles. Therefore, prior to transformation with the plasmids, the *SAT1* genes at both copies of each deletion had to be removed. This removal was possible because the knockout cassette included not only the *SAT1* gene but also a maltose-inducible *FLP* recombinase gene, both of which are flanked by flippase recognition target (FRT) sites (46). Induction of the *FLP* recombinase on maltose medium results in recombination between the FRT sites, thereby deleting the *SAT1* and *FLP* genes. Recombinants that lost both copies of *SAT1* were detected by identification of NAT-sensitive colonies. Introduction of *CHS3*, *CDA2*, *MUM3*, or *SRT1* into the corresponding knockout strains restored Eosin Y staining to the chlamydospores, confirming that the phenotypes are caused by loss of the specific gene function (Fig. 5). We were unable to do the complementation experiment for *rrt8*Δ since the deletion strain failed to grow on the maltose medium used to induce the *FLP* recombinase. Whether the maltose phenotype is a property of the *RRT8* knockout or due to some other change in the strain is unknown. In sum, these results demonstrate that *CHS3*, *CDA2*, *MUM3*, *SRT1*, and probably *RRT8* all

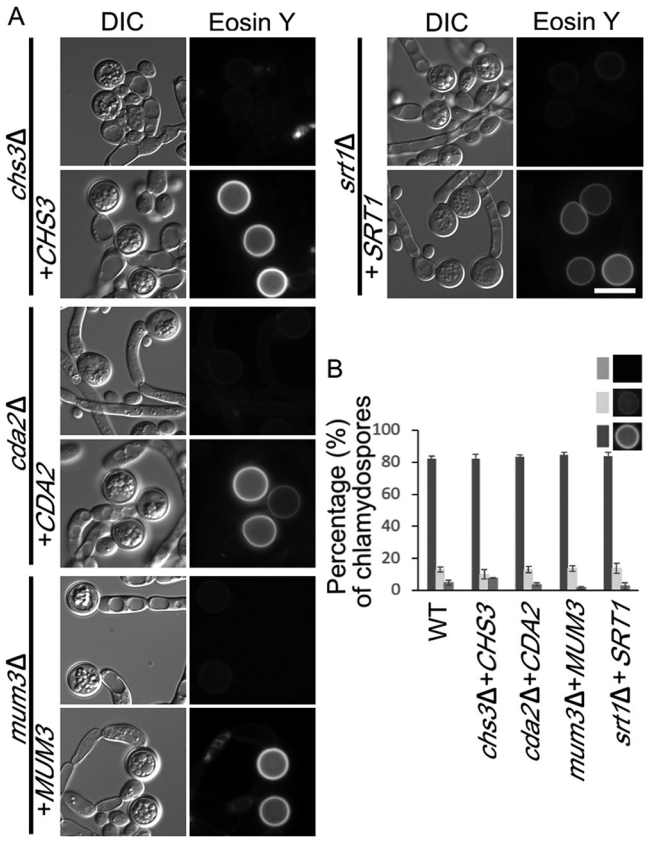

FIG 5 Complementation of the chitosan defect by the wild-type alleles. (A) A wild-type copy of *CHS3*, *CDA2*, *MUM3*, or *SRT1* gene, respectively, was integrated into the corresponding deletion mutant (strains BEM15 to BEM18). Cells were grown on SGlycerol medium, and Eosin Y staining of chlamydospores with or without reintroduction of the wild-type allele was examined. DIC, differential interference contrast. Scale bar, 10 μm. (B) Rescue of Eosin Y staining by the wild-type alleles was quantified as in Fig. 4B..

contribute to formation of a chitosan component of the chlamydospore wall, suggesting that they constitute a conserved machinery mediating chitosan synthesis for incorporation into yeast cell walls.

Ultrastructural analysis identifies a chitosan layer in the chlamydospore wall. The fluorescence images from the Eosin Y staining suggest that chitosan is missing or reduced in the chlamydospore wall of various mutants. Previous ultrastructural studies have revealed that the chlamydospore wall of *C. albicans* is distinct from the hyphal wall in having a darkly staining inner layer of unidentified material underneath what appear to be beta-glucan and mannan layers (42, 53). To examine the ultrastructure of the *C. dubliniensis* chlamydospore wall, cells were stained using osmium and thiocarbohydrazide and examined by electron microscopy (31). Similar to previous reports, the cell walls of wild-type chlamydospores displayed a layer of darkly staining material close to the plasma membrane with outer, lighter layers resembling the walls of the adjacent hyphal cells (Fig. 6).

Given that the chitosan-containing outer ascospore wall of *S. cerevisiae* also stains darkly under these conditions (31), this inner, electron dense material in the chlamydospore wall may be chitosan. Consistent with this possibility and with the Eosin Y fluorescence results, this inner layer was dramatically reduced in both the *chs3*Δ/*chs3*Δ and the *cda2*Δ/*cda2*Δ strains (Fig. 6A). Thus, as in the ascospore wall, chitosan in the chlamydospore wall forms a discrete layer. Again, consistent with the Eosin Y fluorescence results, the chitosan layer appeared reduced or absent in chlamydospores of the *mum3*Δ, *srt1*Δ, and *rrt8*Δ mutants as well (Fig. 6A).

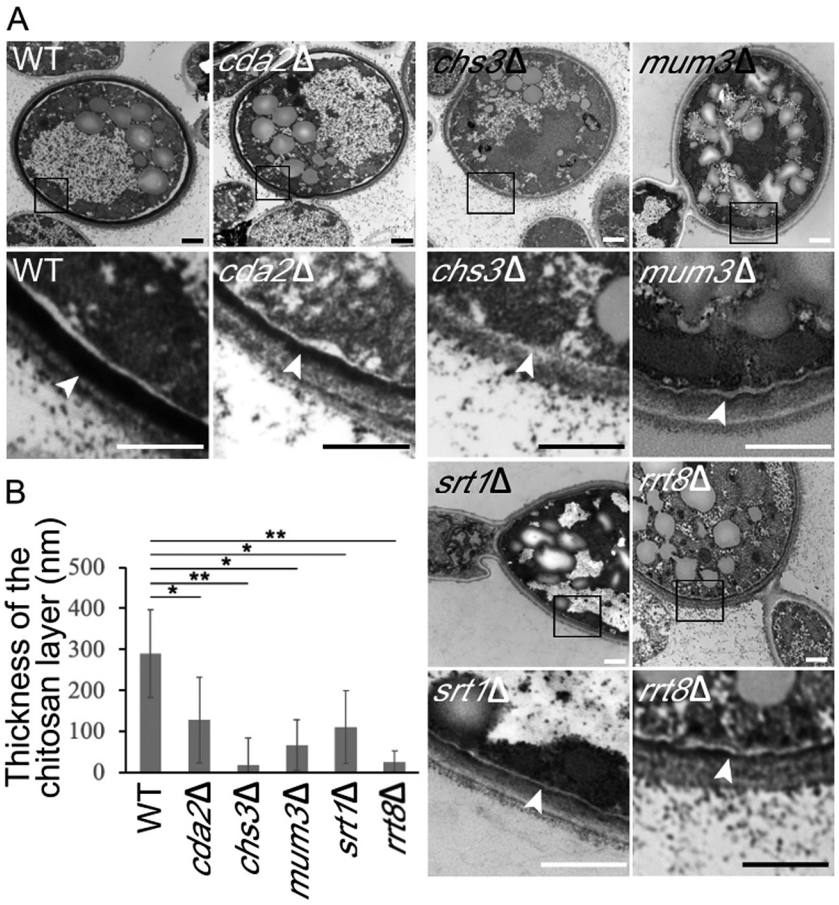

FIG 6 Electron microscopy of the chlamydospore wall of *C. dubliniensis*. (A) Chlamydospores were induced, and cells of different strains were stained with osmium-thiocarbohydrazide: WT (CD1465), *cda2*Δ (BEM7), *chs3*Δ (BEM8), *mum3*Δ (BEM11), *srt1*Δ (BEM14), and *rrt8*Δ (BEM13). For each strain, a pair of images is shown. The lower image is a higher magnification of the boxed region in upper image. Arrowheads indicate the inner cell wall layer. (B) Quantification of the thickness of the chitosan layer in each strain. Data represented are the means of measurements from 20 chlamydospores. The thickness of the chitosan layer was measured at 5 different positions on each chlamydospore. Error bars indicate one standard deviation. One asterisk (*) indicates a significant difference at $P < 0.00005$; two asterisks (**) in indicates $P < 5E{-}10$ (Student *t* test). Scale bar, 500 nm.

The reduction in the chitosan layer visible in the electron micrographs was somewhat variable between chlamydospores in individual strains. Therefore, to measure the effect of the mutants, the thickness of the chitosan layer in the micrographs was measured as an indicator of the amount of chitosan deposited. In each strain, the thickness of the chitosan layer was measured at five locations in 20 different chlamydospores (Fig. 6B). All of the mutants displayed significantly reduced chitosan layers, with the *chs3*Δ strain displaying the strongest phenotype. In sum, the ultrastructural analysis confirms that chitosan is present in a discrete layer of the chlamydospore wall and a conserved set of genes is required for proper formation of this layer.

***C. dubliniensis* Rrt8, Mum3, and Srt1 are all localized on lipid droplets.** In *S. cerevisiae*, the Srt1 and Rrt8/Lds1/Lds2 proteins are localized to lipid droplets, and lipid droplets are associated with the forming spore wall, suggesting some connection between lipid droplets and the assembly of the outer spore wall layers (34–36). *C. albicans* chlamydospores are reported to be rich in neutral lipids and lipid droplets based on both biochemical fractionation and staining with a lipid droplet dye (45, 54). To examine lipid droplets in *C. dubliniensis* chlamydospores, the cells were stained with the lipid droplet dye monodansylpentane (MDH) (55). This treatment revealed a very

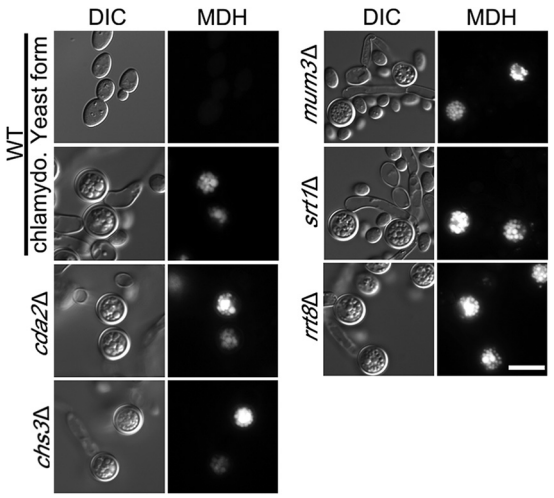

FIG 7 Lipid droplets in chlamydospores. WT cells (CD1465) growing on SGlucose or SGlycerol medium or the indicated *cda2*Δ (BEM7), *chs3*Δ (BEM8), *mum3*Δ (BEM11), *srt1*Δ (BEM14), and *rrt8*Δ (BEM13) mutant strains grown on SGlycerol were stained with MDH to label lipid droplets and visualized using a BFP filter. Scale bar, 10 μm.

high density of lipid droplets within the chlamydospore compared to *C. dubliniensis* cells growing in yeast phase that was not changed in any of the mutant strains (Fig. 7).

The abundance of lipid droplets in the chlamydospore and the connection of the *S. cerevisiae* proteins to lipid droplets led us to examine the localization of the different *C. dubliniensis* proteins. Each gene, under the control of its native promoter, was fused at its 3′ end to a gene encoding a *Candida* codon-optimized red fluorescent protein (yEmRFP) (56). Plasmids containing the fusion genes were then integrated at the *RPS1* locus in the appropriate deletion strains (except for *rrt8*Δ where we were unable to eliminate the *SAT1* gene from the deletion, so a wild-type strain was used).

To confirm that the fusion proteins are functional, the appropriate deletion strains carrying *MUM3*::*yEmRFP* or *SRT1*::*yEmRFP* were examined for the ability of the fusion to rescue the mutant phenotype by staining of chlamydospores with Eosin Y (Fig. 8A). Both fusions restored bright Eosin Y staining indicating that the lipid droplet-localized fusion proteins are functional.

C. dubliniensis cells carrying the different *yEmRFP* fusions were then grown under chlamydospore-inducing conditions, stained with MDH to detect lipid droplets, and examined by fluorescence microscopy. For the *MUM3*, *SRT1*, and *RRT8* fusions, red fluorescence colocalized with the lipid droplet marker in the chlamydospores (Fig. 8B). Red fluorescence at the cell periphery was also visible in the wild-type strain carrying no yEmRFP and so is background fluorescence visible due to the longer exposures necessary to visualize the yEmRFP fusions. Importantly, no background fluorescence was seen at the lipid droplets. The localization of all three proteins suggests that lipid droplets promote chitosan layer formation in *C. dubliniensis*.

DISCUSSION

We report that *C. dubliniensis* efficiently forms chlamydospores when incubated on synthetic medium containing different nonfermentable carbon sources. While the molecular signals that trigger chlamydosporulation are complex (40), nutritional signals are known to be involved and induction by changing carbon sources suggests that central carbon metabolism may play a role. Whether this induction mechanism is unique to *C. dubliniensis* remains to be seen. Though we did not observe chlamydospores with *C. albicans* under our conditions, growth on *N*-acetylglucosamine has been reported to induce chlamydospores in *C. albicans* (57, 58). Previous studies reported that *C. dubliniensis* can form chlamydospores in Staib medium (a seed extract) (59).

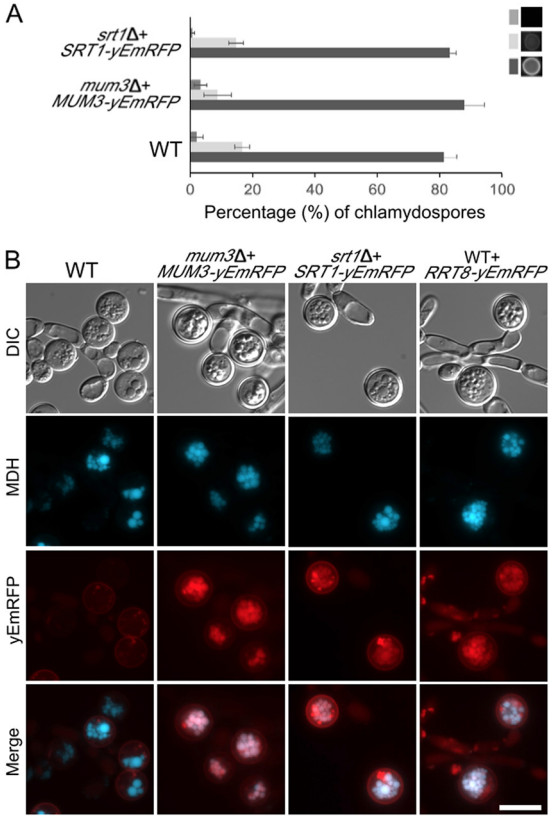

FIG 8 Localization of Cda2, Mum3, Rrt8, and Srt1 in chlamydospores. (A) Eosin Y staining of chlamydospores in WT (CD1465) *mum3*Δ *MUM3-yEMRFP* (BEM20) and *srt1*Δ *SRT1-yEmRFP* (BEM22) strains was quantified as in Fig. 4B. (B) WT (Cd1456) cells expressing no RFP fusion or strains expressing different *MUM3*-, *SRT1*-, or *RRT8-yEmRFP* fusions (BEM20, -21, or -22) were grown on SGlycerol medium, stained with MDH, and visualized through both BFP and RFP filters. Scale bar, 10 μm.

Wild-type *C. albicans* does not form chlamydospores efficiently under these conditions, but deletion of the *C. albicans NRG1* gene leads to chlamydosporulation in Staib medium similar to *C. dubliniensis* (41). The signals triggering chlamydosporulation may be different in SGlyerol and Staib medium, however, since no chlamydospores were seen on SGlycerol when a *C. albicans nrg1* mutant was used (L. D. Bemena, unpublished data).

To create mutant strains in *C. dubliniensis*, we utilized a transient CRISPR-Cas9 system originally developed for *C. albicans* (46). Combining this transient system with the recyclable *SAT1-FLP* cassette allowed us to do multistep strain constructions directly in clinical isolates without the need for auxotrophic markers, greatly accelerating our analysis. That this system works well in both *C. dubliniensis* and *C. albicans* suggests that it will be useful for other *Candida* species as well.

Previously, the chlamydospore wall of *C. albicans* was reported to contain dityrosine based on fluorescence under UV illumination and the observation that deletion of the *CYP56*/*DIT2* gene abolished chlamydospore formation (44). In contrast, using a dityrosine-optimized filter, we find only cytoplasmic fluorescence from chlamydospores of both *C. albicans* and *C. dubliniensis*, and this fluorescence is not altered in *dit1* or *dit2* mutants of *C. dubliniensis*, indicating that the cytoplasmic signal is not dityrosine. While it is possible that the *Candida* species produce a form of dityrosine polymer with different fluorescence characteristics from *S. cerevisiae*, the simplest interpretation of these results is that dityrosine is not a component of the chlamydospore wall in *Candida*.

We show here that chitosan is a major constituent of the previously described dark, inner layer of the *Candida* chlamydospore wall. Chitosan also forms a discrete layer in

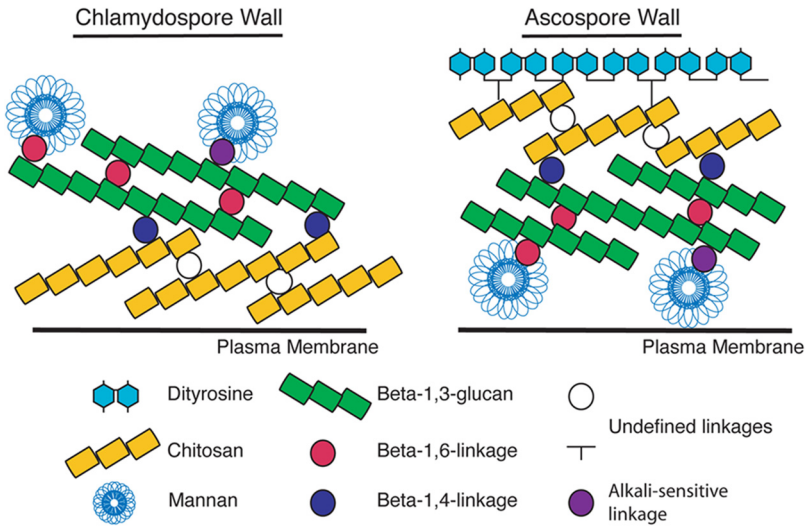

FIG 9 Model for organization of the *C. dubliniensis* chlamydospore and *S. cerevisiae* ascospore walls. The organization of the different layers of the walls is shown with respect to the cell plasma membrane. The linkages between components are based on the known linkages in the vegetative cell wall of *S. cerevisiae* (25). The nature of the cross-links within and between the chitosan and dityrosine layers is unknown.

the *S. cerevisiae* ascospore wall, however, the position of the chitosan layer with respect to other cell wall components is distinct in the two cell walls (Fig. 9). In the ascospore, the chitosan is located toward the outside of the structure, while in the chlamydospore it is on the interior of the wall. In both cases, however, the chitosan is localized adjacent to the beta-glucan components of the wall, suggesting that the presence of the beta-glucan may also be important for organizing the chitosan into a distinct layer. In the ascospore wall, loss of the chitosan layer does not disrupt the shape or integrity of the ascospore but renders the spores sensitive to many environmental insults (29, 31). Similarly, in the chlamydospore wall the chitosan layer is not required for cellular integrity, though whether the chitosan layer also contributes stress resistance is not clear.

Our results reveal a conserved machinery required for chitosan layer synthesis. Multiple chitin synthases are present in both *S. cerevisiae* and *C. dubliniensis*, and yet in both yeasts *CHS3* is uniquely required for synthesis of the chitosan layer of the ascospore and chlamydospore cell walls. Whether this reflects a specific association of this chitin synthase with the chitin deacetylase protein or with some other aspect of Chs3 activity remains to be determined. For example, the Chs3 enzyme might synthesize chitin strands of a chain length or organization that is more amenable to deacetylation. Indeed, *C. albicans* Chs3 has been reported to synthesize shorter chitin fibrils than Chs8 (50).

The lipid droplet-localized proteins Srt1, Rrt8, and Mum3 are required for proper chitosan layer formation in both yeasts. Since these proteins are localized on cytosolic lipid droplets, their effects on chitosan assembly must be somewhat indirect. *MUM3* and *SRT1* encode predicted lipid-synthesizing enzymes. The Mum3 protein is homologous to O-acyltransferase enzymes, and Srt1 is a subunit of a *cis*-prenyltransferase responsible for synthesizing a lipid droplet-localized pool of polyprenols (31, 34). In earlier work, we proposed a model in which Srt1-generated long-chain polyprenols in the lipid droplet that are transferred to the plasma membrane to enhance Chs3 activity (34). It is possible that a similar mechanism occurs during chlamydospore formation. An alternative possibility was recently suggested by nuclear magnetic resonance (NMR) studies of chitosan-containing cell wall preparations from both *S. cerevisiae* and *Cryptococcus neoformans* that revealed neutral lipids are directly incorporated into the

TABLE 1 Strains used in this study

Strain	Genotype	Source or reference
C. dubliniensis		
Cd1465	Wild type	This study
Cd1466	Wild type	This study
Cd1467	Wild type	This study
BEM7	Cd1465, plus *cda2*Δ::*FRT-SAT1*::*FLIP-FRT* /*cda2*Δ:: *FRT-SAT1*::*FLIP-FRT*	This study
BEM8	Cd1465, plus *chs3*Δ:: *FRT-SAT1*::*FLIP-FRT* /*chs3*Δ:: *FRT-SAT1*::*FLIP-FRT*	This study
BEM9	Cd1465, plus *dit1*Δ:: *FRT-SAT1*::*FLIP-FRT* /*dit1*Δ:: *FRT-SAT1*::*FLIP-FRT*	This study
BEM10	Cd1465, plus *dit2*Δ:: *FRT-SAT1*::*FLIP-FRT* /*dit2*Δ:: *FRT-SAT1*::*FLIP-FRT*	This study
BEM11	Cd1465, plus *mum3*Δ:: *FRT-SAT1*::*FLIP-FRT* /*mum3*Δ::*FRT-SAT1*::*FLIP-FRT*	This study
BEM13	Cd1465, plus *rrt8*Δ:: *FRT-SAT1*::*FLIP-FRT* /*rrt8*Δ:: *FRT-SAT1*::*FLIP-FRT*	This study
BEM14	Cd1465, plus *srt1*Δ:: *FRT-SAT1*::*FLIP-FRT* /*srt1*Δ:: *FRT-SAT1*::*FLIP-FRT*	This study
BEM15	Cd1465, plus *cda2*Δ::*FRT*/*cda2*Δ::*FRT RPS1*::P_{CDA2}*CDA2-Clp10-SAT1/RPS1*	This study
BEM16	Cd1465, plus *chs3*Δ::*FRT*/*chs3*Δ::*FRT RPS1*::P_{CHS3}*CHS3-Clp10-SAT1/RPS1*	This study
BEM17	Cd1465, plus *mum3*Δ::*FRT*/*mum3*Δ::*FRT RPS1*::P_{MUM3}*MUM3-Clp10-SAT1/RPS1*	This study
BEM18	Cd1465, plus *srt1*Δ::*FRT*/*srt1*Δ::*FRT RPS1*::P_{SRT1}*SRT1-Clp10-SAT1/RPS1*	This study
BEM19	Cd1465, plus *cda2*Δ::*FRT*/*cda2*Δ::*FRT RPS1*::P_{CDA2}*CDA2-yEmRFP-Clp10-SAT1/RPS1*	This study
BEM20	Cd1465, plus *mum3*Δ::*FRT*/*mum3*Δ::*FRT RPS1*::P_{MUM3}*MUM3-yEmRFP-Clp10-SAT1/RPS1*	This study
BEM21	Cd1465, plus *RPS1*::P_{RRT8}*RRT8*-yEmRFP-*Clp10-SAT1/RPS1*	This study
BEM22	Cd1465, plus *srt1*Δ::FRT/*srt1*Δ::FRT *RPS1*::P_{SRT1}*SRT1-yEmRFP-Clp10-SAT1/RPS1*	This study
C. albicans		
NLC1	*arg4/arg4 his1/his1 leu2/leu2 nrg1*Δ*CmLEU2/nrg1*Δ*CdHIS1*	65

cell wall (16, 60). Thus, the Rrt8, Srt1, and Mum3 proteins may be involved in the synthesis of some lipid component that is then transferred from the lipid droplet to play a structural role during chitosan layer assembly. Further biochemical work will be necessary to clarify how these proteins and their lipid products contribute to the formation of this cell wall structure.

NMR studies suggest that there is a common architecture for chitosan-containing elements in the fungal cell wall from ascomycetes to basidiomycetes (16). Orthologs of the genes described here that underlie formation of chitosan cell wall layers in *Candida* and *Saccharomyces* can be found throughout the fungi. Thus, the similar architecture may reflect a broadly conserved genetic network regulating the synthesis of chitosan-containing cell wall structures in fungi. Given the importance of chitosan to virulence of some pathogenic fungi, the genes described here may be useful targets for antifungal therapies (13).

MATERIALS AND METHODS

Strain and growth conditions. Strains used are listed in Table 1. *C. dubliniensis* strain Cd1465 is derived from a clinical specimen isolated from a patient sample at the Stony Brook hospital. This strain was routinely cultured at 30°C on YPD medium (2% Bacto peptone, 2% dextrose, 1% yeast extract, and 2% agar). *C. dubliniensis* transformants were selected on YPD_NAT (2% Bacto peptone, 2% dextrose, 1% yeast extract, 2% agar, and 400 μg/ml nourseothricin (Werner BioAgents) for nourseothricin-resistant isolates. Synthetic glycerol (SGlycerol) solid medium (1.7% yeast nitrogen base without amino acids, 2% agar, and 0.1 M glycerol) was used to induce chlamydospores, as described below.

Induction of chlamydospores. To induce chlamydospore formation in *C. dubliniensis*, wild-type and mutant strains were inoculated in 5 ml of YPD liquid and incubated at 30°C with shaking at 220 rpm for overnight. A suspension of 1×10^7 cells/ml was prepared from the overnight culture. The cell suspension was then diluted 100 times and 1 ml was spread on a SGlycerol plate. Excess liquid was removed by pipetting, and the plates were left to dry at room temperature. All the plates were incubated in 30°C for 24 h. The chlamydospores were collected by adding 500 μl of distilled water to the plate and gently scraping the surface of the plate with a glass rod. To induce chlamydospores in *C. albicans*, a slice was made in a plate of corn meal agar with Tween 80 (Hardy Diagnostics, USA). 100 μl of an overnight culture in YPD medium was inoculated into the slice, and a cover slip placed over the line of inoculation. The plates were incubated at 25°C for 5 days.

CRISPR-Cas9 mutagenesis in *C. dubliniensis*. To create knockout mutations in *C. dubliniensis*, we adapted a CRISPR/CAS9 system developed for *C. albicans* (61). The pV1093 vector carries both Cas9 and single-guide RNA (sgRNA) expression cassettes (61). Guide RNAs targeting specific genes were designed using the CCTop (CRISPR/Cas9 target online) program (62). The *CAS9* gene expression cassette and the sgRNA scaffold were amplified separately from pV1093 using the primers BLD1 and BLD2. The sgRNA

scaffold contains the *SNR52* promoter was assembled by the single-joint PCR method (63). Briefly, three-DNA synthesis step was used to generate the sgRNA cassette. The first step consists to amplify by PCR the *SNR52* promoter and sgRNA scaffold using gene-specific flanking primers (Table 2) and internal chimeric primers (BLD3 and BLD4). Twenty complementary bases overlapped and specified the sgRNA of each gene to be knocked out. For the second step, both components were fused by primer extension, relying upon annealing of the complementary chimeric primer extensions. The third step consists of amplifying the joined product with nested primers (BLD5 and BLD6) to yield the sgRNA cassette.

The FLP recombination target sequence target (FRT) and the *SAT1* cassette both encoded in pGR_NAT vector, were flanked by ~20-bp homology to the 5′ and 3′ regions of the gene to be knocked out. This fragment was PCR amplified and used as the gene deletion construct (46). The oligonucleotides used in this study are listed in Table 2. PCR amplifications were conducted using Ex Taq in accordance with the manufacturer's instructions (TaKaRa Bio, Inc.).

For the mutagenesis, PCR products for transformation were purified and concentrated with a commercial PCR purification kit (Qiagen, Germantown, MD). The deletion constructs (3 μg) were cotransformed with the CdCAS9 cassette (1 μg) and the sgRNA cassette (1 μg) using the lithium acetate transformation method (64). At least five independent homozygous deletion strains were tested for each mutant.

Rescue of mutant strains. For each mutant, to confirm that the observed phenotypes were due to the deletion, an integrating plasmid carrying the wild-type gene was constructed. Clp10-SAT (a gift from N. Dean) was used as the vector. To construct the complementing plasmids, Clp10 was amplified as two separate fragments by PCR. The first fragment, amplified with BLD121 and OKZ67, contains the ApaI site at the one end and part of the Amp locus at the other end. The second fragment, amplified with BLD123 and OKZ68, harbors an overlapping fragment of the Amp locus at one end and an XhoI site at the other end. Each gene of interest was amplified by PCR from *C. dubliniensis* genomic DNA with 15-bp homologous sequence to the region of Clp10 carrying the ApaI or XhoI sites at the opposite ends. *CDA2* was amplified with BLD104 and BLD105, *CHS3* with BLD97 and BLD11, *MUM3* with BLD112 and BLD113, and *SRT1* with BLD116 and BLD117. The three fragments were fused by Gibson Assembly (BioLabs) and transformed into *Escherichia coli*. All of the plasmids used in this study are listed in Table 3.

In order to rescue the mutant strains, we first recycled the selectable marker *SAT1*. To allow the recycling, the mutant strains were plated on YPM (2% Bacto peptone, 2% maltose, 1% yeast extract, 2% agar) to induce expression of the FLP recombinase (47) and then replica plated to YPD_NAT medium. Colonies that became sensitive to nourseothricin were selected for transformation with the integrating plasmid carrying the corresponding wild-type gene. The plasmids were linearized by digestion with NcoI before transformation into the mutant strains by lithium acetate transformation method (64) with modifications. Briefly, fresh overnight cultures (12 h to 16 h) were diluted 1:50 and incubated for ~6 h (optical density at 600 nm of 5.0. The cells were harvested, washed once with H_2O and once with 100 mM lithium acetate (LiOAc), and resuspended in 100 μl of LiOAc (100 mM). We used a transformation mixture composed of 240 μl of polyethylene glycol (50%), 32 μl of LiOAc (1 M), 33 μl of linearized plasmid (~30 μg), and 5 μl of ssDNA, to which 100 μl of cell suspension was added. The mixture tube was incubated for overnight at 30°C. The next day, the tube was heat shocked at 44°C for 15 min. The cells were harvested and washed with YPD and then resuspended in 1 ml. The suspension was incubated at 30°C with shaking for 6 h. After the incubation period, the cells were harvested and spread on YPD_NAT plates. The plates were incubated at 30°C, and colonies were visible after 2 days.

Localization of Cda2, Mum3, Rrt8, and Srt1. To localize the proteins of interest, plasmids were constructed by creating fusion genes that express C-terminal fusions to yEmRFP. First, the Clp10 vector was digested with KpnI and XhoI. Next, the gene of interest was amplified without the stop codon, using genomic DNA obtained from strain Cd1465. The yEmRFP fragment was amplified by PCR using yEpGAP-Cherry vector (56) as the template. As described above, the three fragments were fused by Gibson assembly. The plasmids were linearized by digestion with NcoI and transformed into the nourseothricin-sensitive mutants by the lithium acetate transformation method.

CFW/Eosin Y staining. Chlamydospores were collected and washed with 1 ml of McIlvaine's buffer (0.2 M Na_2HPO_4, 0.1 M citric acid [pH 6.0]), followed by staining with 30 μl of Eosin Y disodium salt (Sigma; 5 mg/ml) in 500 μl of McIlvaine's buffer for 10 min at room temperature in the dark. Chlamydospores were then washed twice in McIlvaine's buffer to remove residual dye and resuspended in 200 μl of McIlvaine's buffer. One microliter of a 1-mg/ml Calcofluor White (CFW) solution (Sigma) was then added to the Eosin Y-stained cells before transfer to microscope slides. The fluorescence of CFW and Eosin Y stains was then examined using DAPI (4′,6′-diamidino-2-phenylindole) and fluorescein isothiocyanate filter sets, respectively.

MDH staining of lipid droplets. To stain lipid droplets in chlamydospores with monodansylpentane (MDH; Abgent), chlamydospores collected as described above were washed once with 1× PBS, followed by incubation in 1 ml of PBS containing 100 mM MDH for 15 min in 37°C. Chlamydospores were then washed twice with 1× PBS and examined by fluorescence microscopy using a BFP optimized filter set to visualize MDH fluorescence.

Microscopy. All images were collected on a Zeiss Axio-Imager microscope using a Hamamatsu ER-G camera and Zen 3.0 software. Different exposure times used for the different fluors as follows: Eosin Y, 200 ms; CFW, 5 ms; dityrosine, 2s; DAPI, 2s; yEmRFP, 2s; and MDH, 10 ms.

Transmission electron microscopy. Chlamydospores were collected as described above and stained for electron microscopy using osmium and thiocarbohydrazide staining as described previously (31). Briefly, chlamydospores were fixed by resuspension in 3% glutaraldehyde in cacodylate buffer, for 1 h, washed once in 0.1 M cacodylate buffer (pH 7.4), and then resuspended in 1% osmium tetroxide

TABLE 2 Oligonucleotide primers used in this study

Primer	Key feature	Sequence (5′–3′)
BLD1	CaCas9 forward	ATCTCATTAGATTTGGAACTTGTGGGTT
BLD2	CaCas9 reverse	TTCGAGCGTCCCAAAACCTTCT
BLD3	*SNR52* forward	AAGAAAGAAAGAAAACCAGGAGTGAA
BLD4	sgRNA reverse	ACAAATATTTAAACTCGGGACCTGG
BLD5	*SNR52* NGG	GCGGCCGCAAGTGATTAGACT
BLD6	sgRNA NGG	GCAGCTCAGTGATTAAGAGTAAAGATGG
BLD17	*CDA2* FLP forward	CGGTTTAATAGTCATTTAATAAAAACTCTTGAAATTCTTATCAAATAAACTAATCATTCTTCAATTACCATAAAGGGAACAAAAGCTGGG
BLD18	*CDA2* FLP reverse	CAACACTAAATTCTTCTTTGTAACCACCTACCTACCTACATACATACATACATACAATACAAGAATTTTTGTATTGATCTCTAGAACTAGTGGATCTG
BLD19	*DIT1 SNR52* reverse	GATGATTTACATGGAAAGGCCAAATTAAAAATAGTTTACGCAAGTC
BLD20	*DIT1* sgRNA forward	GCCTTTCCATGTAAATCATCGTTTTAGAGCTAGAAATAGCAAGTTAAA
BLD23	*DIT1* FLP forward	CGTTGAATTCAAATACAAGTAGTAATACCACGGTTGATACAGATTCGTTTGAACAAAAGCAACAACAAATATTGAAGCTAAAGGGAACAAAAGCTGGG
BLD24	*DIT1* FLP reverse	CGTTTTCACTCTCGTCACAGTTGGCCACAACCTATCGTCAGAAGAAGAAACAATAATCCAACGGAACAAACCTCTAGAACTAGTGGATCTG
BLD25	*DIT1* upstream verification forward	GGCTGCAATTTCCCCAAAAG
BLD26	*DIT1* downstream verification reverse	GCCAGAGTAGCCAACAAGTTA
BLD27	*CDA2* upstream verification forward	TTCCGGTGGTAATTTTGATGAGA
BLD29	*DIT1* midgene verification reverse	GGTCCCATGATGATGACAGG
BLD30	*CDA2* midgene verification reverse	TTTGTTGAGAGCATCCCACC
BLD31	*CDA2* downstream verification forward	GACTCGGTGCAATCTTGTCA
BLD36	*MUM3* sgRNA forward	GTAGTCCAAATATTTACTTCGTTTTAGAGCTAGAAATAGCAAGTTAAA
BLD37	*MUM3 SNR52* reverse	GAAGTAAATATTTGGACTACCAAATTAAAAATAGTTTACGCAAGTC
BLD38	*MUM3* FLP forward	GGCGACACTACCGATGCCAATCCCGCTGTGGTAGTAAGTAACCATGCATCTTTAGCGGACTGCTTTGTTATTCTAAAGGGAACAAAAGCTGGG
BLD39	*MUM3* FLP reverse	CTACCGGATTCAAAGAGATGAAAGTAGTAAATCAAGAATTTATAGTTTACCTATAGGTAGGATTCAAGAGAACCTCTAGAACTAGTGGATCTG
BLD40	*MUM3* upstream verification forward	CAGCATTTGAATAAGGTAAA
BLD41	*MUM3* midgene verification reverse	TGTCCCTGTAACGTTGCTCC
BLD42	*MUM3* downstream verification reverse	GGGAGATAGGTTTACTGATC
BLD43	*RRT8* sgRNA forward	GGTACGGAGTCGTTGCACTTGTTTTAGAGCTAGAAATAGCAAGTTAAA
BLD44	*RRT8 SNR52* reverse	AAGTGCAACGACTCCGTACCCAAATTAAAAATAGTTTACGCAAGTC
BLD45	*RRT8* FLP forward	CCAATCTTCTAGACGTGGGCTAAAGGCACATGCAAGATACTTTAAGTTGAAAGGGTTTCTGCGTAGCGACTAAAGGGAACAAAAGCTGGG
BLD46	*RRT8* FLP reverse	GCAGGTTGGTTGTTGAGGTCTAAGTTTAGTAGCAGCAATGAAGGTGGAGTTGCTGCTGGGTTTGGATGTGCTCTAGAACTAGTGGATCTG
BLD47	*RRT8* upstream verification forward	GTGGGCCCAATCATTGTCTTG
BLD48	*RRT8* midgene verification reverse	TGATAAATGGGAACAGCTCG
BLD49	*RRT8* downstream verification reverse	CGGGTGAAATCTTGACCAAC
BLD50	*SRT1* sgRNA forward	TGGGAAAGAACCTCGTGTCCGTTTTAGAGCTAGAAATAGCAAGTTAAA
BLD51	*SRT1 SNR52* reverse	GGACACGAGGTTCTTTCCCACAAATTAAAAATAGTTTACGCAAGTC
BLD52	*SRT1* FLP forward	CAAAATAAGTTAACCAGAAAAGCAATACTTGTCTTGTAAGTCGGAAAGCTTTTTACAAGATCATAGTTCCAGTAAAGGGAACAAAAGCTGGG
BLD53	*SRT1* FLP reverse	GAATCTATTCATGACAACTTTGCATATTCTAGCTAAAATACAAAATACAATCGTAAAGCAAGGCTCTAGAACTAGTGGATCTG
BLD54	*SRT1* upstream verification forward	GGATTAATTGTCGAGTGGCA
BLD55	*SRT1* midgene verification reverse	GTAATACTGGTGGAATAAC
BLD56	*SRT1* downstream verification reverse	TAAATAACCAGGTAGACTTG
BLD64	*CHS3* sgRNA forward	AAGGTGGACGTGAAGTTTATGTTTTAGAGCTAGAAATAGCAAGTTAAA
BLD65	*CHS3 SNR52* reverse	ATAAACTTCACGTCCACCTTCAAATTAAAAATAGTTTACGCAAGTC
BLD66	*CHS3* FLP forward	CCCTTGCATTAACACCAAAACTTATAGACAACAGAAACATTAGTCTTTTTTGTTTTCTACATTTATTCCTCTAAAGGGAACAAAAGCTGGG
BLD67	*CHS3* FLP reverse	GTACAATGCATGCAATAAACAAGGCAGAAATTTGAAATATTCTGGAGCCTCTATGTTATAAAGCAGCGTTGCTCTAGAACTAGTGGATCTG
BLD68	*CHS3* upstream verification forward	GTTTTCAATTACAATTAATC
BLD69	*CHS3* midgene verification reverse	CATAATCGTTAATTTCATCG
BLD70	*CHS3* downstream verification reverse	TTTGTGTTTGTAAGAGATTC

(Continued on next page)

TABLE 2 (Continued)

Primer	Key feature	Sequence (5′–3′)
BLD71	*CDA2* sgRNA forward	ATCCGATCCATTTATTATGGGTTTTAGAGCTAGAAATAGCAAGTTAAA
BLD72	*CDA2 SNR52* reverse	CCATAATAAATGGATCGGATCAAATTAAAAATAGTTTACGCAAGTC
BLD73	*CDA2* verification reverse	CATGAATTTAGATTGAAGTC
BLD74	*DIT2* sgRNA forward	TTAGTGCTCATGGAGAATTGGTTTTAGAGCTAGAAATAGCAAGTTAAA
BLD75	*DIT2 SNR52* reverse	CAATTCTCCATGAGCACTAACAAATTAAAAATAGTTTACGCAAGTC
BLD76	*DIT2* FLP forward	GCACAGATAACCCTTTTGCTATTTGAGAACCATCCGGGTGATACTAGCCTTGCTCTTTCCTCTTAAACAAGTAAAGGGAACAAAAGCTGGG
BLD77	*DIT2* FLP reverse	GTGAGTGTGGGGTGTTTTCTGTTAGCAAACGCAAGTTATATACTATATGGTATGTACTGCATTCTTCATTCCTCTAGAACTAGTGGATCTG
BLD78	*DIT2* upstream verification forward	GACAATGAAATTTCCAAGACTCC
BLD79	*DIT2* midgene verification reverse	GGGCAACAACATCTCGGTATAG
BLD80	*DIT2* downstream verification reverse	AAATGCTTAGCTTACAGGGG
BLD97	Clp10_*CHS3* forward	CGATACCGTCGACCTCGAGGACAGACAGAGAGAGAGATCAGAGATTGAA
BLD104	Clp10_*CDA2* forward	CACTATAGGGCGAATTGGGTACCCGAAATTTAAAGAGACAATTGAAAAAATTACAAGGAG
BLD105	Clp10_*CDA2* reverse	GGGAACAAAAGCTGGGTACCTCATTTTGGGAAAGTTTTAATATAATCAATACCACC
BLD111	Clp10_*CHS3* reverse	CAAAAGCTGGGTACCGGGCCCTCAACCAGACCCCGAAGATGATCC
BLD112	Clp10_*MUM3* forward	CTTATCGATACCGTCGACCTCGAGATGGAATTCATTGAGCATTTAGGAGTCAAGC
BLD113	Clp10_*MUM3* reverse	CAAAAGCTGGGTACCGGGCCCCTACAGAGCTACAGAAAAATCATCTTGCAATATACG
BLD116	Clp10_*SRT1* forward	TACCGTCGACCTCGAGACAATTATAAATGTTTTCATTAGTGTTGGTAGTGTATCATATGC
BLD117	Clp10_*SRT1* reverse	GGGAACAAAAGCTGGGTACCGGGCCCTTAAATAACTGATGTAGCAGGTGGAGGG
BLD118	Clp10_*SRT1* verification	GGACAATCTCTTGTTTTTACC
BLD121	Clp10 first half forward	CCCGGTACCCAGCTTTTGTTCCCTTTAGTG
BLD123	Clp10 second half reverse	CTCGAGGTCGACGGTATCG
BLD125	Clp10_*RRT8* forward	CGATACCGTCGACCTCGAGATTGTTAATGGGACCACTAGGGGTG
BLD126	Clp10_*RRT8* reverse	CAAAAGCTGGGTACCGGGCCCTCAGATGGTATTTGTAGCAGTCTTTGGG
BLD142	yEmRFP forward	ATGGTTTCAAAAGGTGAAGAAGATAATATGGC
BLD143	Clp10_*CDA2*_yEmRFP reverse	TCTTCACCTTTTGAAACCATTTTTGGGAAAGTTTTAATATAATCAATACCACCAACAC
BLD144	Clp10_*MUM3*_yEmRFP reverse	CTTCTTCACCTTTTGAAACCATCAGAGCTACAGAAAAATCATCTTGCAATATACG
BLD145	Clp10_*RRT8*_yEmRFP reverse	CTTCTTCACCTTTTGAAACCATGATGGTATTTGTAGCAGTCTTTGGGG
BLD146	Clp10_*SRT1*_yEmRFP reverse	CTTCTTCACCTTTTGAAACCATAATAACTGATGTAGCAGGTGGAGGG
BLD148	yEmRFP reverse	CGATACCGTCGACCTCGAGTTATTTATATAATTCATCCATACCACCAGTTGAATGTCT
BLD153	Clp10_*RRT8*_yEmRFP verification	TGTTACGACAAAAGGCTCAA
BLD154	Clp10_*CDA2_SAT1* verification	TACATTTATATAAAACCAGT
BLD155	Clp10_*CDA2*_yEmRFP verification	GATGAAAAATAATAAAGGTT
BLD156	Clp10_*MUM3*_yEmRFP verification	ACCGGTAGATCTGTTGATCA
BLD157	Clp10_*SRT1*_yEmRFP verification	GGAGTTATTATAGAACTATT
OKZ67	Clp10 first half reverse	GTATTCAACATTTCCGTGTCG
OKZ68	Clp10 second half forward	CGACACGGAAATGTTGAATAC

TABLE 3 Plasmids used in this study

Plasmid	Name	Key feature	Source or reference
pNAT	pNAT	P_{URA3}*URA3 SAT1*	46
pV1093	pV1093	*CaCas9/SAT1* flipper *ENO1*	61
Clp10-SAT	Clp10-SAT	*CaRPS1 SAT1*	N. Dean
yEpGAP_Cherry	yEpGAP_Cherry	*URA3* yEmRFP	56
pLB1	Clp10_*CDA2*	*CaRPS1* P_{CDA2}*CDA2 SAT1*	This study
pLB2	Clp10_*CHS3*	*CaRPS1* P_{CHS3}*CHS3 SAT1*	This study
pLB3	Clp10_*MUM3*	*CaRPS1* P_{MUM3}*MUM3 SAT1*	This study
pLB4	Clp10_*RRT8*	*CaRPS1* P_{RRT8}*RRT8 SAT1*	This study
pLB5	Clp10_*SRT1*	*CaRPS1* P_{SRT1}*SRT1 SAT1*	This study
pLB6	Clp10_*CDA2*_yEmRFP	*CaRPS1* P_{CDA2}*CDA2* yEmRFP *SAT1*	This study
pLB7	Clp10_*MUM3*_yEmRFP	*CaRPS1* P_{MUM3}*MUM3* yEmRFP *SAT1*	This study
pLB8	Clp10_*RRT8*_yEmRFP	*CaRPS1* P_{RRT8}*RRT8* yEmRFP*SAT1*	This study
pLB9	Clp10_*SRT1*_yEmRFP	*CaRPS1* P_{SRT1}*SRT1* yEmRFP *SAT1*	This study

and 1% potassium ferricyanide in cacodylate buffer for 30 min at room temperature. Chlamydospores were then washed four times in dH_2O, resuspended in 1% thiocarbohydrazide in water, and incubated for 5 min at room temperature, followed by one wash in dH_2O and an additional 5-min incubation in 1% osmium tetroxide and 1% potassium ferricyanide. The chlamydospores were then incubated in saturated uranyl acetate for 2 h and dehydrated through a graded series of acetone washes. The dehydrated samples were then treated with 100% propylene oxide for 10 min, embedded in Epon 812, and sectioned, and images were collected on an FEI BioTwin microscope at 80 kV.

Statistics. Data are presented as means ± the standard errors of the indicated numbers of independent samples. Statistical significance was determined with Student *t* test (two tailed, heteroscedastic) using Microsoft Excel software. Differences between the analyzed samples were considered significant at $P < 0.05$.

ACKNOWLEDGMENTS

We thank Neta Dean for reagents and advice, members of the Konopka and Neiman labs for helpful discussions, and Nancy Hollingsworth for comments on the manuscript.

This study was supported by NIH grant GM072540 to A.M.N. and NIH grants R01GM116048 and R01AI047837 to J.B.K.

REFERENCES

1. Free SJ. 2013. Fungal cell wall organization and biosynthesis. Adv Genet 81:33–82. https://doi.org/10.1016/B978-0-12-407677-8.00002-6.
2. Garcia-Rubio R, de Oliveira HC, Rivera J, Trevijano-Contador N. 2019. The fungal cell wall: *Candida*, *Cryptococcus*, and *Aspergillus* species. Front Microbiol https://doi.org/10.3389/fmicb.2019.02993.
3. Cortes JCG, Curto MA, Carvalho VSD, Perez P, Ribas JC. 2019. The fungal cell wall as a target for the development of new antifungal therapies. Biotechnol Adv 37:107352. https://doi.org/10.1016/j.biotechadv.2019.02.008.
4. Denning DW. 2003. Echinocandin antifungal drugs. Lancet 362:1142–1151. https://doi.org/10.1016/S0140-6736(03)14472-8.
5. Georgopapadakou NH, Tkacz JS. 1995. The fungal cell wall as a drug target. Trends Microbiol 3:98–104. https://doi.org/10.1016/s0966-842x(00)88890-3.
6. Selitrennikoff CP, Nakata M. 2003. New cell wall targets for antifungal drugs. Curr Opin Invest Drugs 4:200–205.
7. Brown HE, Esher SK, Alspaugh JA. 2020. Chitin: a "hidden figure" in the fungal cell wall. Curr Top Microbiol Immunol 425:83–111. https://doi.org/10.1007/82_2019_184.
8. Kollar R, Reinhold BB, Petrakova E, Yeh HJ, Ashwell G, Drgonova J, Kapteyn JC, Klis FM, Cabib E. 1997. Architecture of the yeast cell wall: $\beta(1\rightarrow6)$-glucan interconnects mannoprotein, $\beta(1\rightarrow)$3-glucan, and chitin. J Biol Chem 272:17762–17775. https://doi.org/10.1074/jbc.272.28.17762.
9. Baker LG, Specht CA, Donlin MJ, Lodge JK. 2007. Chitosan, the deacetylated form of chitin, is necessary for cell wall integrity in *Cryptococcus neoformans*. Eukaryot Cell 6:855–867. https://doi.org/10.1128/EC.00399-06.
10. Briza P, Ellinger A, Winkler G, Breitenbach M. 1988. Chemical composition of the yeast ascospore wall: the second outer layer consists of chitosan. J Biol Chem 263:11569–11574. https://doi.org/10.1016/S0021-9258(18)37997-3.
11. Christodoulidou A, Bouriotis V, Thireos G. 1996. Two sporulation-specific chitin deacetylase-encoding genes are required for the ascospore wall rigidity of *Saccharomyces cerevisiae*. J Biol Chem 271:31420–31425. https://doi.org/10.1074/jbc.271.49.31420.
12. Matsuo Y, Tanaka K, Matsuda H, Kawamukai M. 2005. *cda1*$^+$, encoding chitin deacetylase is required for proper spore formation in *Schizosaccharomyces pombe*. FEBS Lett 579:2737–2743. https://doi.org/10.1016/j.febslet.2005.04.008.
13. Baker LG, Specht CA, Lodge JK. 2011. Cell wall chitosan is necessary for virulence in the opportunistic pathogen *Cryptococcus neoformans*. Eukaryot Cell 10:1264–1268. https://doi.org/10.1128/EC.05138-11.
14. Hole CR, Lam WC, Upadhya R, Lodge JK. 2020. *Cryptococcus neoformans* chitin synthase 3 plays a critical role in dampening host inflammatory responses. mBio 11:e03373-19. https://doi.org/10.1128/mBio.03373-19.
15. Lam WC, Upadhya R, Specht CA, Ragsdale AE, Hole CR, Levitz SM, Lodge JK. 2019. Chitosan biosynthesis and virulence in the human fungal pathogen *Cryptococcus gattii*. mSphere 4:e00644. https://doi.org/10.1128/mSphere.00644-19.
16. Chrissian C, Lin CP, Camacho E, Casadevall A, Neiman AM, Stark RE. 2020. Unconventional constituents and shared molecular architecture of the melanized cell wall of *Cryptococcus neoformans* and spore wall of *Saccharomyces cerevisiae*. J Fungi 6:329. https://doi.org/10.3390/jof6040329.
17. Neiman AM. 2005. Ascospore formation in the yeast *Saccharomyces cerevisiae*. Microbiol Mol Biol Rev 69:565–584. https://doi.org/10.1128/MMBR.69.4.565-584.2005.
18. Neiman AM. 2011. Sporulation in the budding yeast *Saccharomyces cerevisiae*. Genetics 189:737–765. https://doi.org/10.1534/genetics.111.127126.
19. Briza P, Ellinger A, Winkler G, Breitenbach M. 1990. Characterization of a DL-dityrosine-containing macromolecule from yeast ascospore walls. J Biol Chem 265:15118–15123. https://doi.org/10.1016/S0021-9258(18)77231-1.

20. Ishihara S, Hirata A, Nogami S, Beauvais A, Latge JP, Ohya Y. 2007. Homologous subunits of 1,3-β-glucan synthase are important for spore wall assembly in *Saccharomyces cerevisiae*. Eukaryot Cell 6:143–156. https://doi.org/10.1128/EC.00200-06.
21. Lynn RR, Magee PT. 1970. Development of the spore wall during ascospore formation in *Saccharomyces cerevisiae*. J Cell Biol 44:688–692. https://doi.org/10.1083/jcb.44.3.688.
22. Tachikawa H, Bloecher A, Tatchell K, Neiman AM. 2001. A Gip1p-Glc7p phosphatase complex regulates septin organization and spore wall formation. J Cell Biol 155:797–808. https://doi.org/10.1083/jcb.200107008.
23. Briza P, Breitenbach M, Ellinger A, Segall J. 1990. Isolation of two developmentally regulated genes involved in spore wall maturation in *Saccharomyces cerevisiae*. Genes Dev 4:1775–1789. https://doi.org/10.1101/gad.4.10.1775.
24. Whelan WL, Ballou CE. 1975. Sporulation in D-glucosamine auxotrophs of *Saccharomyces cerevisiae*: meiosis with defective ascospore wall formation. J Bacteriol 124:1545–1557. https://doi.org/10.1128/JB.124.3.1545-1557.1975.
25. Orlean P. 2012. Architecture and biosynthesis of the *Saccharomyces cerevisiae* cell wall. Genetics 192:775–818. https://doi.org/10.1534/genetics.112.144485.
26. Shaw JA, Mol PC, Bowers B, Silverman SJ, Valdivieso MH, Duran A, Cabib E. 1991. The function of chitin synthases 2 and 3 in the *Saccharomyces cerevisiae* cell cycle. J Cell Biol 114:111–123. https://doi.org/10.1083/jcb.114.1.111.
27. Silverman SJ. 1989. Similar and different domains of chitin synthases 1 and 2 of *S. cerevisiae*: two isozymes with distinct functions. Yeast 5:459–467. https://doi.org/10.1002/yea.320050605.
28. Pammer M, Briza P, Ellinger A, Schuster T, Stucka R, Feldmann H, Breitenbach M. 1992. *DIT101* (*CSD2*, *CAL1*), a cell cycle-regulated yeast gene required for synthesis of chitin in cell walls and chitosan in spore walls. Yeast 8:1089–1099. https://doi.org/10.1002/yea.320081211.
29. Christodoulidou A, Briza P, Ellinger A, Bouriotis V. 1999. Yeast ascospore wall assembly requires two chitin deacetylase isozymes. FEBS Lett 460:275–279. https://doi.org/10.1016/s0014-5793(99)01334-4.
30. Briza P, Eckerstorfer M, Breitenbach M. 1994. The sporulation-specific enzymes encoded by the *DIT1* and *DIT2* genes catalyze a two-step reaction leading to a soluble LL-dityrosine-containing precursor of the yeast spore wall. Proc Natl Acad Sci U S A 91:4524–4528. https://doi.org/10.1073/pnas.91.10.4524.
31. Coluccio A, Bogengruber E, Conrad MN, Dresser ME, Briza P, Neiman AM. 2004. Morphogenetic pathway of spore wall assembly in *Saccharomyces cerevisiae*. Eukaryot Cell 3:1464–1475. https://doi.org/10.1128/EC.3.6.1464-1475.2004.
32. Felder T, Bogengruber E, Tenreiro S, Ellinger A, Sa-Correia I, Briza P. 2002. Dtrlp, a multidrug resistance transporter of the major facilitator superfamily, plays an essential role in spore wall maturation in *Saccharomyces cerevisiae*. Eukaryot Cell 1:799–810. https://doi.org/10.1128/ec.1.5.799-810.2002.
33. Gomez-Esquer F, Rodriguez-Pena JM, Diaz G, Rodriguez E, Briza P, Nombela C, Arroyo J. 2004. *CRR1*, a gene encoding a putative transglycosidase, is required for proper spore wall assembly in *Saccharomyces cerevisiae*. Microbiology (Reading) 150:3269–3280. https://doi.org/10.1099/mic.0.27314-0.
34. Hoffmann R, Grabińska K, Guan Z, Sessa WC, Neiman AM. 2017. Long-chain polyprenols promote spore wall formation in *Saccharomyces cerevisiae*. Genetics 207:1371–1386. doi:10.1534/genetics.117.300322. https://doi.org/10.1534/genetics.117.300322.
35. Lin CP, Kim C, Smith SO, Neiman AM. 2013. A highly redundant gene network controls assembly of the outer spore wall in *Saccharomyces cerevisiae*. PLoS Genet 9:e1003700. https://doi.org/10.1371/journal.pgen.1003700.
36. Ren J, Pei-Chen Lin C, Pathak MC, Temple BR, Nile AH, Mousley CJ, Duncan MC, Eckert DM, Leiker TJ, Ivanova PT, Myers DS, Murphy RC, Brown HA, Verdaasdonk J, Bloom KS, Ortlund EA, Neiman AM, Bankaitis VA. 2014. A phosphatidylinositol transfer protein integrates phosphoinositide signaling with lipid droplet metabolism to regulate a developmental program of nutrient stress-induced membrane biogenesis. Mol Biol Cell 25:712–727. https://doi.org/10.1091/mbc.E13-11-0634.
37. Staib P, Morschhauser J. 2007. Chlamydospore formation in *Candida albicans* and *Candida dubliniensis*: an enigmatic developmental programme. Mycoses 50:1–12. https://doi.org/10.1111/j.1439-0507.2006.01308.x.
38. Sudbery P, Gow N, Berman J. 2004. The distinct morphogenic states of *Candida albicans*. Trends Microbiol 12:317–324. https://doi.org/10.1016/j.tim.2004.05.008.
39. Martin SW, Douglas LM, Konopka JB. 2005. Cell cycle dynamics and quorum sensing in *Candida albicans* chlamydospores are distinct from budding and hyphal growth. Eukaryot Cell 4:1191–1202. https://doi.org/10.1128/EC.4.7.1191-1202.2005.
40. Bottcher B, Pollath C, Staib P, Hube B, Brunke S. 2016. *Candida* species rewired hyphae developmental programs for chlamydospore formation. Front Microbiol 7:1697. https://doi.org/10.3389/fmicb.2016.01697.
41. Staib P, Morschhauser J. 2005. Differential expression of the *NRG1* repressor controls species-specific regulation of chlamydospore development in *Candida albicans* and *Candida dubliniensis*. Mol Microbiol 55:637–652. https://doi.org/10.1111/j.1365-2958.2004.04414.x.
42. Jansons VK, Nickerson WJ. 1970. Induction, morphogenesis, and germination of the chlamydospore of *Candida albicans*. J Bacteriol 104:910–921. https://doi.org/10.1128/JB.104.2.910-921.1970.
43. Staib P, Morschhauser J. 1999. Chlamydospore formation on Staib agar as a species-specific characteristic of *Candida dubliniensis*. Mycoses 42:521–524. https://doi.org/10.1046/j.1439-0507.1999.00516.x.
44. Melo NR, Moran GP, Warrilow AG, Dudley E, Smith SN, Sullivan DJ, Lamb DC, Kelly DE, Coleman DC, Kelly SL. 2008. CYP56 (Dit2p) in *Candida albicans*: characterization and investigation of its role in growth and antifungal drug susceptibility. Antimicrob Agents Chemother 52:3718–3724. https://doi.org/10.1128/AAC.00446-08.
45. Hernandez-Cervantes A, Znaidi S, van Wijlick L, Denega I, Basso V, Ropars J, Sertour N, Sullivan D, Moran G, Basmaciyan L, Bon F, Dalle F, Bougnoux ME, Boekhout T, Yang Y, Li Z, Bachellier-Bassi S, d'Enfert C. 2020. A conserved regulator controls asexual sporulation in the fungal pathogen *Candida albicans*. Nat Commun 11:6224. https://doi.org/10.1038/s41467-020-20010-9.
46. Min K, Ichikawa Y, Woolford CA, Mitchell AP. 2016. *Candida albicans* gene deletion with a transient CRISPR-Cas9 system. mSphere 1:e00130-16. https://doi.org/10.1128/mSphere.00130-16.
47. Reuss O, Vik A, Kolter R, Morschhauser J. 2004. The *SAT1* flipper, an optimized tool for gene disruption in *Candida albicans*. Gene 341:119–127. https://doi.org/10.1016/j.gene.2004.06.021.
48. Suda Y, Rodriguez RK, Coluccio AE, Neiman AM. 2009. A screen for spore wall permeability mutants identifies a secreted protease required for proper spore wall assembly. PLoS One 4:e7184. https://doi.org/10.1371/journal.pone.0007184.
49. Henar Valdivieso M, Duran A, Roncero C. 1999. Chitin synthases in yeast and fungi. EXS 87:55–69. https://doi.org/10.1007/978-3-0348-8757-1_4.
50. Lenardon MD, Whitton RK, Munro CA, Marshall D, Gow NA. 2007. Individual chitin synthase enzymes synthesize microfibrils of differing structure at specific locations in the *Candida albicans* cell wall. Mol Microbiol 66:1164–1173. https://doi.org/10.1111/j.1365-2958.2007.05990.x.
51. Mio T, Yabe T, Sudoh M, Satoh Y, Nakajima T, Arisawa M, Yamada-Okabe H. 1996. Role of three chitin synthase genes in the growth of *Candida albicans*. J Bacteriol 178:2416–2419. https://doi.org/10.1128/jb.178.8.2416-2419.1996.
52. Murad AM, Lee PR, Broadbent ID, Barelle CJ, Brown AJ. 2000. Clp10, an efficient and convenient integrating vector for *Candida albicans*. Yeast 16:325–327. https://doi.org/10.1002/1097-0061(20000315)16:4<325::AID-YEA538>3.0.CO;2-#.
53. Shannon JL. 1981. Scanning and transmission electron microscopy of *Candida albicans* chlamydospores. J Gen Microbiol 125:199–203. https://doi.org/10.1099/00221287-125-1-199.
54. Jansons VK, Nickerson WJ. 1970. Chemical composition of chlamydospores of *Candida albicans*. J Bacteriol 104:922–932. https://doi.org/10.1128/JB.104.2.922-932.1970.
55. Currie E, Guo X, Christiano R, Chitraju C, Kory N, Harrison K, Haas J, Walther TC, Farese RV, Jr. 2014. High-confidence proteomic analysis of yeast LDs identifies additional droplet proteins and reveals connections to dolichol synthesis and sterol acetylation. J Lipid Res 55:1465–1477. https://doi.org/10.1194/jlr.M050229.
56. Keppler-Ross S, Noffz C, Dean N. 2008. A new purple fluorescent color marker for genetic studies in *Saccharomyces cerevisiae* and *Candida albicans*. Genetics 179:705–710. https://doi.org/10.1534/genetics.108.087080.
57. Strippoli V, Simonetti N. 1975. Specific induction of chlamydospore formation in *Candida albicans* by *N*-acetyl-D-glucosamine. Experientia 31:130–131. https://doi.org/10.1007/BF01924719.

58. Torosantucci A, Cassone A. 1983. Induction and morphogenesis of chlamydospores in an agerminative variant of *Candida albicans*. Sabouraudia 21:49–57. https://doi.org/10.1080/00362178385380081.
59. Palige K, Linde J, Martin R, Bottcher B, Citiulo F, Sullivan DJ, Weber J, Staib C, Rupp S, Hube B, Morschhauser J, Staib P. 2013. Global transcriptome sequencing identifies chlamydospore specific markers in *Candida albicans* and *Candida dubliniensis*. PLoS One 8:e61940. https://doi.org/10.1371/journal.pone.0061940.
60. Chrissian C, Camacho E, Kelly JE, Wang H, Casadevall A, Stark RE. 2020. Solid-state NMR spectroscopy identifies three classes of lipids in *Cryptococcus neoformans* melanized cell walls and whole fungal cells. J Biol Chem 295:15083–15096. https://doi.org/10.1074/jbc.RA120.015201.
61. Vyas VK, Barrasa MI, Fink GR. 2015. A *Candida albicans* CRISPR system permits genetic engineering of essential genes and gene families. Sci Adv 1:e1500248. https://doi.org/10.1126/sciadv.1500248.
62. Stemmer M, Thumberger T, Del Sol Keyer M, Wittbrodt J, Mateo JL. 2015. CCTop: an intuitive, flexible, and reliable CRISPR/Cas9 target prediction tool. PLoS One 10:e0124633. https://doi.org/10.1371/journal.pone.0124633.
63. Yu JH, Hamari Z, Han KH, Seo JA, Reyes-Dominguez Y, Scazzocchio C. 2004. Double-joint PCR: a PCR-based molecular tool for gene manipulations in filamentous fungi. Fungal Genet Biol 41:973–981. https://doi.org/10.1016/j.fgb.2004.08.001.
64. Walther A, Wendland J. 2003. An improved transformation protocol for the human fungal pathogen *Candida albicans*. Curr Genet 42:339–343. https://doi.org/10.1007/s00294-002-0349-0.
65. Noble SM, French S, Kohn LA, Chen V, Johnson AD. 2010. Systematic screens of a *Candida albicans* homozygous deletion library decouple morphogenetic switching and pathogenicity. Nat Genet 42:590–598. https://doi.org/10.1038/ng.605.